Anal. Chem. **2003,** *75,* 5137−5145

Development of High-Sensitivity Ion Trap Ion Mobility Spectrometry Time-of-Flight Techniques: A High-Throughput Nano-LC-IMS-TOF Separation of Peptides Arising from a *Drosophila* Protein Extract

Sunnie Myung,[†] Young Jin Lee,[†,‡] Myeong Hee Moon,[†] John Taraszka,[†] Rena Sowell,[†] Stormy Koeniger,[†] Amy E. Hilderbrand,[†] Stephen J. Valentine,[§] Lucy Cherbas,[||] Peter Cherbas,[||] Thomas C. Kaufmann,[||] David F. Miller,[||] Yehia Mechref,[†] Milos V. Novotny,[†] Michael A. Ewing,[⊥] C. Ray Sporleder,[†] and David E. Clemmer*[,†]

Department of Chemistry, Indiana University, Bloomington, Indiana 47405, Beyond Genomics, 40 Bear Hill Road, Waltham, Massachusetts 02451, Department of Biology, Indiana University, Bloomington, Indiana 47405, and Department of Chemistry, Rose Hulman University, Terra Haute, Indiana 47803

A linear octopole trap interface for an ion mobility time-of-flight mass spectrometer has been developed for focusing and accumulating continuous beams of ions produced by electrospray ionization. The interface improves experimental efficiencies by factors of ∼50−200 compared with an analogous configuration that utilizes a three-dimensional Paul geometry trap (Hoaglund-Hyzer, C. S.; Lee, Y. J.; Counterman, A. E.; Clemmer, D. E. ***Anal. Chem.*** **2002,** ***74,*** **992−1006). With these improvements, it is possible to record nested drift (flight) time distributions for complex mixtures in fractions of a second. We demonstrate the approach for several well-defined peptide mixtures and an assessment of the detection limits is given. Additionally, we demonstrate the utility of the approach in the field of proteomics by an on-line, three-dimensional nano-LC-ion mobility-TOF separation of tryptic peptides from the *Drosophila* proteome.**

There is a significant interest in developing methods for analyzing complex mixtures of biomolecules—especially proteins.[1,2] With this in mind, multidimensional separation techniques such as two-dimensional gel electrophoresis and multidimensional liquid chromatographic (LC) separations are being developed and combined with techniques of mass spectrometry (MS).[3,4] An issue that emerges with these combinations is the rate at which samples can be introduced into the MS instrument. Most mass spectrometers require at most only a few seconds to acquire data; however, most separation strategies require much longer times to separate components. This mismatch in timing presents a need to develop faster separations that can effectively feed components into the mass spectrometer.

One such high-speed separation is ion mobility spectrometry (IMS). IMS is an analytical method that was developed in the 1970s to detect trace analytes, such as explosives.[5] In the past few years, several groups have coupled IMS techniques to MS instruments in order to characterize complex mixtures.[6] In this approach, a packet of gas-phase ions is introduced into a well-defined drift region and the time required for the ions to travel through a buffer gas under the influence of an applied electric field is recorded. Individual components of complex mixtures can be resolved on the basis of differences in the shapes and charge states of the ions that are produced.[7] A significant feature of the IMS separation (as applied to complex mixtures) is the short time

* Corresponding author. E-mail: clemmer@indiana.edu.

† Department of Chemistry, Indiana University.

‡ Present address: Molecular Structure Facility, University of California, Davis, CA 95616.

§ Beyond Genomics.

|| Department of Biology, Indiana University.

⊥ Rose Hulman University.

(1) Yates, J. R. III. *J. Mass Spectrom.* **1998**, *33*, 1.

(2) Mann, M.; Hendrickson, R. C.; Pandey, A. *Annu. Rev. Biochem.* **2001**, *70*, 437.

(3) For recent examples of LC−MS and 2DE-MS methods see: (a) Mann, M.; Hojrup, P.; Roepstorff, P. *Biol. Mass Spectrom.* **1993**, *22*, 338. (b) Yates, J. R.; Speicher, S.; Griffin, P. R.; Hunkapiller, T. *Anal. Biochem.* **1993**, *32*, 397. (c) Gygi, S. P.; Corthals, G. L.; Zhang, Y.; Rochon, Y.; Aebersold, R. *Proc. Natl. Acad. Sci. U.S.A.* **2000**, *97*, 17. (d) Lee, E. D.; Muck, W.; Henion, J. D.; Covey, T. R. *J. Chromatogr.* **1988**, *458*, 313. (e) Niessen, W. M. A. *J. Chromatogr., A* **1998**, *794*, 407. (f) Smith, R. D.; Udseth, H. R.; Wahl, J. H.; Goodlett, D. R.; Hofstadler, S. A. *Methods Enzymol.* **1996**, *271*, 448. (g) Goodlett, D. R.; Wahl, J. H.; Udseth, H. R.; Smith, R. D. *J. Microcolumn Sep.* **1993**, *5*, 57. (h) Starkey, J. A.; Mechref, Y.; Byun, C. K.; Steinmetz, R.; Fuqua, J. S.; Pescovitz, O. H.; Novotny, M. V. *Anal. Chem.* **2002**, *74*, 5998, and references therein.

(4) For a recent review, see: Abersold, F.; Goodlett, D. R. *Chem. Rev.* **2001**, *101*, 269.

(5) Hill, H. H.; Siems, W. F.; St. Louis, R. H.; McMinn, D. G. *Anal. Chem.* **1990**, *62*, 1201A.

(6) For recent examples, see: (a) Taraszka, J. A.; Counterman, A. E.; Clemmer, D. E. *Fresenius J. Anal. Chem.* **2001**, *369*, 234. (b) Valentine, S. J.; Counterman, A. E.; Clemmer, D. E. *J. Am. Soc. Mass Spectrom.* **1998**, *10*, 1188. (c) Guevremont, R.; Barnett, D. A.; Purves, R. W.; Vandermey, P. J. *Anal. Chem.* **2000**, *72*, 4577.

(7) General information and application of IMS in obtaining structural information: (a) Bower, M. T.; Kemper, P. R.; Helden, G. V.; Koppen, P. A. M. V. *Science* **1993**, *260*, 1446. (b) Helden, G. V.; Hsu, M. T.; Gotts, N.; Bowers, M. T. *J. Phys. Chem.* **1993**, *97*, 8182. (c) Helden, G. V.; Wyttenbach, T.; Bowers, M. T. *Int. J. Mass Spectrom. Ion Processes* **1995**, *146/147*, 349. (d) Gotts, N. G.; Helden, G. V.; Bowers, M. T. *Int. J. Mass Spectrom. Ion Processes* **1995**, *149/150*, 217. (e) Clemmer, D. E.; Jarrold, M. F. *J. Mass Spectrom.* **1997**, *32*, 577. (f) Clemmer, D. E.; Hudgins, R. R.; Jarrold, M. F. *J. Am. Chem. Soc.* **1995**, *117*, 10141. (g) Dugourd, Ph.; Hudgins, R. R.; Clemmer, D. E.; Jarrold, M. F. *Rev. Sci. Instrum.* **1997**, *68*, 1122.

10.1021/ac030107f CCC: $25.00
Published on Web 08/23/2003

required to separate components (usually milliseconds), thus, reducing mixture complexity while introducing components for MS analysis very rapidly.

The potential value of high-speed separation approaches such as IMS can be seen by considering an *efficiency factor* (E_f).[8] Following Hill's work, we define $E_f = Nt^{-1}$, where N corresponds to the theoretical plate parameter used in separation science and t is the time of the separation. Values of E_f for IMS separations can be very high. For example, from a recently published high-resolution IMS separation,[9] we calculate $N \sim 375\,180$ at $t = 0.0155$ s, leading to $E_f = 2.4 \times 10^7$ plates·s^{-1}. Typical values for low-resolution separations, obtained from injected ion drift tube designs,[10] give values of $N = 3500$ at $t = 0.002$ s, leading to $E_f = 1.75 \times 10^6$ plates·s^{-1}. These values are much higher than those derived for other separation methods (e.g., Hill reported $E_f = 14$ plates·s^{-1} for high-performance LC and $E_f = 500$ for capillary electrophoresis).[8] In the end, the advantages in efficiency factor that arise for IMS come about because ions have high mobilities through the low-density buffer gas and thus require very short separation times, usually milliseconds (or shorter).[8]

The millisecond time scale associated with the IMS separation provides another opportunity—it is intermediate between the longer times (seconds to minutes) required for LC and detection times (μs) required in the time-of-flight (TOF) mass spectrometer. In principle, it is possible to separate components by LC, softly ionize them by electrospray ionization (ESI),[11,12] and then disperse ions on the basis of differences in their mobilities prior to the MS measurement—without discarding any ions! In practice, however, to date such an approach has been of limited use because ions are lost, thus severely limiting the sensitivity of this approach for a routine three-dimensional analysis.

There are two key factors that limit the sensitivity associated with incorporating the mobility separation with LC−MS. First, the transmission efficiency of ions in to and out of the drift tube can lead to significant signal loss. The efficiency of ion transmission out of the drift tube can be estimated by considering the volume of the ion packet, after ions have diffused through the instrument, along with the dimensions of the drift tube exit. We have recently addressed this issue by developing a high-field focusing element at the exit of the drift tube.[13] This approach improves transmission by more than 1 order of magnitude compared to previous designs.[10] The issue associated with the efficiency of transmitting ions into the entrance of the drift tube is more difficult to assess; however, variations of focusing conditions and hole sizes suggest that losses at the entrance are less significant than at the exit.

The second factor that significantly limits the efficiency of combining mobility separations with ESI-MS emerges because of the continuous nature of the ESI source and the pulsed nature of the IMS separation. Ions from the continuous source are gated into the drift tube in discrete packets (~1.0−100 μs in duration) that are much shorter than the longest drift time that is recorded in the experiment (1.0−100.0 ms); therefore, most of the continuous ion beam is discarded between experiments.[14]

We have previously improved duty factors by inclusion of Paul geometry ion trap.[14] In this paper, we describe the development of an octopole trap interface for IMS-TOF experiments. The inclusion of the octopole provides a dramatic improvement in signal. Compared with the Paul trapping geometries, the linear octopole configuration provides factors of ~50−200 times higher signals. It appears that the ability to store ions along the linear axis of the octopole significantly improves the ability to accumulate ions in packets from the continuous source. Below, we describe the experimental configuration in detail and present several studies of well-defined mixtures of peptides to examine the detection limits of this approach. With the improvements that are found it is now routine to carry out multidimensional nano-LC-IMS-TOF separations on complex systems. We demonstrate this by showing several data sets for a separation involving all of the soluble tryptic peptides from the *Drosophila* proteome. We also provide brief descriptions of (a) new limitations that arise as a result of these improvements, (b) possible solutions to these issues, and (c) the outlook for using this approach to study complex mixtures.

EXPERIMENTAL SECTION

General Information. The IMS-MS instrument design that is used for this work has been discussed in detail elsewhere.[10,15] Only a brief description of this approach is provided here. Instead, we provide a detailed description of the modifications associated with including a linear octopole trap. Briefly, IMS-MS experiments are carried out as follows. Peptides are directly infused (from a syringe pump or a nano-LC) into a home-built ESI source. Desolvated ions are extracted into the high-vacuum portion of the instrument, where they are focused into (and accumulated) a linear geometry octopole trap (described below). Mobility-MS experiments are initiated by periodically ejecting the accumulated packet of ions from the trap into a drift tube. The drift tube is a 50.3-cm-long chamber filled with ~1.5 Torr helium buffer gas. Ions travel across the tube and through the gas under the influence of a uniform electric field that is created by applying appropriate potentials to a series of equally spaced electrodes inside the chamber. Different ions are separated based on differences in their mobilities through the buffer gas. Compact ions have higher mobilities than larger ions and thus appear at shorter drift times.[7e] ESI often produces a distribution of charge states;[16] it is often the case that the high charge states have higher mobilities than low charge states because these ions experience a greater drift force. Typically the drift tube resolving power for the instrument used here ranges from 20 to 30 for low charge state peptide ions.

Upon exiting the drift tube, ions are focused into the source region of a reflectron geometry TOF mass spectrometer. Here, high-repetition, high-voltage pulses (synchronous with the initial ejection pulse from the octopole trap) are used to initiate MS

(8) Asbury, G. R.; Hill, H. H., Jr. *J. Microcolumn Sep.* **2000**, *12*, 172.
(9) Srebalus, C. A.; Li, J.; Marshall, W. S.; Clemmer, D. E. *Anal. Chem.* **1999**, *71*, 3918.
(10) Hoaglund-Hyzer, C. S.; Lee, Y. J.; Counterman, A. E.; Clemmer, D. E. *Anal. Chem.* **2002**, *74*, 992.
(11) Fenn, J. B.; Mann, M.; Meng, C. K.; Wong, S. F.; Whitehouse, C. M. *Science* **1989**, *246*, 64.
(12) Karas, M.; Hillenkamp, F. *Anal. Chem.* **1988**, *60*, 2299.
(13) Our original report suggested that the improvement in signal was a factor of ~5−10. Subsequent studies show ≥10× improvement: Lee, Y. J.; Hoaglund-Hyzer, C. S.; Taraszka, J. A.; Zientara, G. A.; Counterman, A. E.; Clemmer, D. E. *Anal. Chem.* **2001**, *73*, 3549−3555.
(14) Hoaglund-Hyzer, C. S.; Valentine, S. J.; Clemmer, D. E. *Anal. Chem.* **1997**, *69*, 4156.
(15) Lee, Y. J.; Hoaglund-Hyzer, C. S.; Srebalus-Barnes, C. A.; Hilderbrand, A. E.; Valentine, S. J.; Clemmer, D. E. *J. Chromatogr., B* **2002**, *782*, 343−351.
(16) (a) Wong, S. F.; Meng, C. K.; Fenn, J. B. *J. Phys. Chem.* **1988**, *92*, 546. (b) Mann, M,; Meng, C. K.; Fenn, J. B. *Anal. Chem.* **1989**, *61*, 1702.

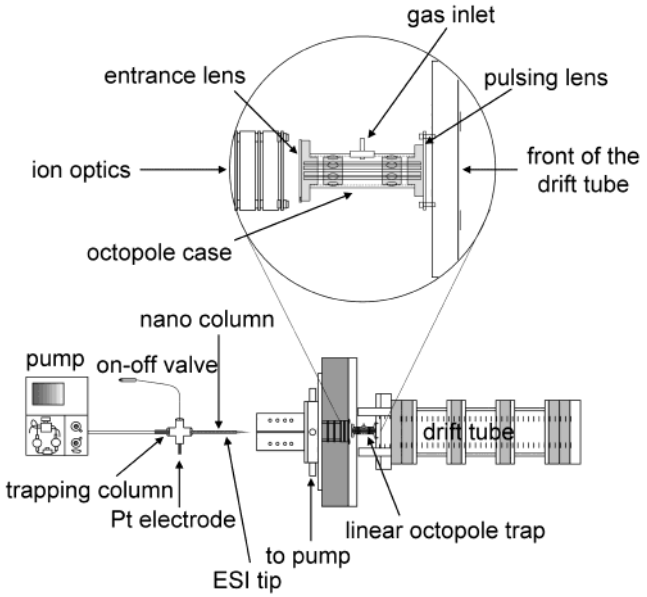

Figure 1. Schematic diagram showing the home-built nano-LC, ESI, linear ion trap, and drift tube assembly used in this work. The ion trap is situated between the focusing elements of the ESI source and the drift tube and mounts to the front flange of the drift tube. The eight octopole rods are fixed in position by macor standoff mounts as shown. The assembly is encased and incorporates an inlet for introducing buffer gases. Packets of ions that accumulate in the trap are ejected by pulsing a negative potential (>30 μs in duration) at the end of the trap. The remaining portions of the IMS-TOF instrument used in this study have been described previously (See refs 10 and 15 for details).

measurements. Flight times in the evacuated flight tube of the mass spectrometer are much shorter than the millisecond residence times of ions inside the drift tube. Thus, it is possible to record flight time distributions as ions exit the drift tube in what we have referred to as a nested fashion, described in detail previously.[17] Ions are detected in the mass spectrometer using a home-built microchannel plate/anode assembly. Typically, the resolving power of the m/z measurement in this instrument is 400−1400.[10]

The instrument is also equipped with an on-axis detector. In this case, ions pass through the source region and are detected. This detector is useful for initial ion focusing and determining the duty cycle associated with the TOF measurements (~0.5−3% in these experiments). The data acquisition system and electronics, which includes the pulsing electronics, time-to-digital converters, and programmable delay generators, were constructed in-house and have been described previously.[17]

Octopole Trap Interface. A schematic diagram showing the linear octopole ion trap interface is shown in Figure 1. The trap is situated immediately after the focusing optics associated with the ion source and is mounted to the front of the drift tube. The trap consists of eight 2.70-mm-diameter stainless steel rods that are each 78.4 mm long. The rods are mounted equidistant from one another on a circle using two macor mounting block standoffs. In this configuration, the octopole inner diameter is 5.40 mm. The system of rods and standoffs is enclosed in a stainless steel case that incorporates a gas inlet and stainless steel entrance and exit lenses. An rf generator (with frequency of 1.6 MHz and V_{pp} =780; see additional discussion below) is used to apply potentials to the octopole rods. To trap the continuous beam, ions are decelerated as they enter the trap. This is accomplished by operating the trap entrance voltage (and dc bias of the octopole rods) within several volts of the source. The exit lens of the trap is operated at a slightly higher potential. Helium buffer gas (1−5 mTorr) is introduced through a leak valve (Granville Phillips, Boulder, CO) to the trap to aid in cooling the ions. Ions trapped inside the octopole can be extracted and injected into the drift tube by applying negative pulsing voltage to the exit lens.

Optimizing Conditions for Trapping Ions. A number of different operating conditions and experimental configurations were tested during the development of the octopole/drift tube combination, including the following: (1) the position of octopole relative to other focusing optics between the source and the drift tube; (2) the helium pressure inside the trap; (3) the applied rf rod potentials and frequencies and the end-cap biases. In the end, a number of configurations appear suitable and offer substantial advantages relative to three-dimensional Paul traps. The primary advantages associated with the increased trapping efficiency of the octopole device appear to arise from fundamental advantages, including the following: (1) the higher order multipole has a wider effective potential well;[18] (2) ions are stored along an axis (rather than at a point) such that more ions can be accumulated before ions begin leaking from the trap. An additional advantage may be associated with the focusing nature of the octopole; this device is simple to align with the drift tube entrance orifice, and injection of ions into the small entrance orifice requires relatively little adjustment of focusing optics. Trapping frequencies were varied over a range of 1.1−1.7 MHz, and the applied trapping potentials were varied from 100 to 1000 V_{pp}. While the optimal trapping conditions depend on the system that is being studied, we typically operate at a frequency of 1.6 MHz and V_{pp} = 780. A range of helium pressures was also tested. The optimum helium pressure inside the trap is estimated to be 1−5 mTorr.

During an ion mobility time-of-flight experiment, the trapping of the ions in the axial direction of the linear trap was accomplished by raising the potential on the entrance lens (30 V above the drift tube voltage), the rf dc bias (24 V above the drift tube potential), and the pulsing lens (~15 V above the entrance lens). The higher potential on the pulsing lens was necessary in order to block leaking ions from entering the drift tube as mentioned above. The pulsing lens was pulsed with a negative 70 V with a pulse width of 100 μs, which was significantly greater than the 1−10-μs pulse width that was used for a Paul trap

(17) Hoaglund, C. S.; Valentine, S. J.; Sporleder, C. R.; Reilly, J. P.; Clemmer, D. E. *Anal. Chem.* **1998**, *70*, 2236.

(18) For a discussion of multipole devices see, for example: (a) Voyksner, R. D.; Lee, H. *Rapid Commun. Mass Spectrosc.* **1999**, *13*, 1427. (b) Senko, M. W.; Hendrickson, C. L.; Pasa-Tolic, L.; Marto, J. A.; White, F. M.; Guan, S.; Marshall, A. G. *Rapid Commun. Mass Spectrom.* **1996**, *10*, 1824. (c) Wang, Y.; Shi, S. D.-H.; Hendrickson, C. L.; Marshall, A. G. *Int. J. Mass Spectrom.* **2000**, *198*, 113. (d) Campbell, J. M.; Collings, B. A.; Douglas, D. J. *Rapid Commun. Mass Spectrum.* **1998**, *12*, 1463. (e) Teloy, E.; Gerlich, D. *Chem. Phys.* **1974**, *4*, 417. (f) Teloy, E. In *Electronics and Atomic Collisions*; Watel, G., Ed.; North-Holland: Amsterdam, 1978; Vol. 591. (g) Houle, F. A.; Gerlich, D.; Lee, Y. T. *J. Chem. Phys.* **1981**, *75*, 2153. (h) Ervin, K. M.; Armentrout, P. B. J. *Chem. Phys.* **1987**, *86*, 2659. (i) Tolmachev, A. V.; Chernushevich, I. V.; Dodonov, A. F.; Standing, K. G. *Nucl. Instrum, Methods Phys. Res.* **1997**, *124*, 112. (j) Tosi, P.; Fontana, G.; Longano, S.; Bassi, D.; *Int. J. Mass Spectrom. Ion Processes* **1989**, *93*, 95, and references therein.

configuration; however, this was much lower than the millisecond time scale that was associated with the mobility distribution.

Sample Preparation. The experiments described below utilize three different types of samples: (1) a mixture of peptides obtained upon tryptic digestion of albumin; (2) a standard peptide mixture; (3) tryptic peptides that were derived from soluble proteins extracted from the *Drosophila* (either the Kc cell line or from the head of an adult fly). A mixture of tryptic peptides of albumin (horse, purity of ≥90%, Sigma, St. Louis, MO) was prepared by a procedure that has been outlined previously.[15] Disulfide bonds were reduced and alkylated, prior to digestion with 2% (w/w) trypsin (bovine pancreas, TPCK treated; Sigma, St. Louis, MO) at 37 °C for 20 h. To reduce disulfide bonds, dithiothreitol (DTT) was used at a 1:40 mole ratio. After 2-h incubation at 37 °C, iodoacetamide was added at a 1:80 mole ratio and incubated in darkness on ice for 2 h more. To quench the reaction, cysteine was added at a 1:40 mole ratio and the reaction was allowed to proceed at room temperature for 30 min. Solutions containing Met-enkephalin (98% purity, Sigma), angiotensin I (98% purity, Sigma), angiotensin II (98% purity, Sigma), and susbstance P (98% purity, Sigma) were prepared over a range of concentrations extending from 1.0 to 243 $\mu g \cdot mL^{-1}$. All solutions were prepared in water (EM Science, HPLC grade) with 2% acetic acid added to enhance the nanospray signal. A nanospray flow rate of 50 $nL \cdot min^{-1}$ from a homemade capillary nanotip was used. The pulled tip was connected to a PEEK microcross as described elsewhere in order to supply electrospray voltage of 1.9 kV.[19]

Several types of complex protein mixtures from the *Drosophila* were used. Proteins from a pool of *Drosophila* Kc cell lines induced by ecdysone hormone[20] and another pool in which a hormone was applied were grown in CCM3 media (Hyclone, Logan, UT). The proteins were extracted by sonicating the cells for 5 min followed by the extraction of the proteins onto a phosphate-buffered saline solution containing 0.1 mM of DTT and 0.1 mM of phenylmethanesulfonyl fluoride (PMSF). The proteins were then reduced and alkylated (as mentioned above), digested with trypsin, and labeled with heavy (CD_3CO) and light (CH_3CO) isotope acetyl groups at the N-terminus and lysine residues using the global internal standard technology (GIST) method.[21] These labeled peptides were mixed together in equal amounts, and the peptides were lyophilized. These peptides were analyzed using a commercial LC system as described below.

In addition, we describe an experiment involving a single wild-type fly head of Oregon-R, *Drosophila melanogaster*. In this experiment, heads from wild-type *D, melanogaster* were obtained from flies that were grown at 22 °C on standard *Drosophila* media[22] that was supplemented with baker's yeast. Proteins from a single head were extracted into 100 μL of a phosphate-buffered saline solution containing 4.0 M urea and 0.1 mM of PMSF using a micromortar and pestle. A Bradford assay indicated that typically 5 μg of protein was obtained. This was followed by reduction and alkylation as mentioned above. Finally the sample was digested with 2% (w/w) trypsin (bovine pancreas, TPCK treated; Sigma) at 37 °C for 20 h as described previously.[15] After digestion, samples were desalted using Oasis HLB (Waters) sample extraction cartridges. Peptides were eluted from the cartridges using 250 μL of a 60:40 acetonitrile/water solution and 150 μL of a 90:10 acetonitrile/water solution. Eluted peptides were dried on a centrifugal concentrator and stored at −80 °C until further analysis.

Nano-LC Separations. Reversed-phase LC separation of the GIST labeled ecdysone induced and normal *Drosophila* proteome samples was performed using a LC-Packing Ultimate nano LC system and a C_{18} column (PepMap C_{18}, 3 μm (100-Å pore), 75 μm × 150 mm; Dionex, Sunnyvale, CA). A binary gradient with solvent A (water, 0.1% formic acid) and solvent B (acetonitrile, 0.1% formic acid) was used as the chromatographic mobile phase with the following gradient sequence: B was maintained at 5% for 30 min, and then it was slowly increased to 45% during the next 30 min, followed by rapid ramping to 100% over the last 10 min of the gradient at a flow rate of 180 $nL \cdot min^{-1}$ for an on-line separation using a homemade pulled capillary nanospray tip. A total concentration of 1 $\mu g \cdot \mu L^{-1}$ mixture sample was injected to the LC system through 1-μL loop and IMS−MS distributions were recorded for every 10 s.

A brief description of the complete homemade nano-LC system of the separation is as follows: using the same mobile phase as described above, the gradient was maintained constant for 1 min at 100% A, was slowly increased to 25% B over 55 min, and then increased to 100% B over the next 50 min at a flow rate of 250 $nL \cdot min^{-1}$. As shown in Figure 1, the nano-LC system consisted of a LC-Packing Ultimate pump (Dionex), a homemade nano-column (75 μm × 150 mm) and a packed trapping column (100 μm × 15 mm). The tip at the end of the 75-μm-id fused capillary (Polymicro Technology LLC, Phoenix, AZ) was pulled with a flame and packed with methanol slurry of 5-μm, 100-Å Magic C18AQ (Microm BioResourses Inc., Auburn, CA) without a frit at a constant pressure (1000 psi) of He. Immediately before the analytical column, we utilize a homemade packed trapping column for cleanup of sample materials. The trapping column was packed in a silica tubing (100-μm inner diameter) with an integral frit from New Objective Inc. (Woburn, MA) for 1.5 cm by using 5-μm, 200-Å Magic C18 slurries.

Nomenclature for LC-IMS-MS Data Sets. An important consideration in the design of this experimental approach is the time scale of each analysis. In the present data, the time scales are such that individual dimensions can be acquired in a nested fashion, as described previously for two-dimensional IMS-MS measurements.[10,17] The positions of individual peaks can be described by a simple nomenclature that incorporates the concept of the nested measurement. We report retention times (t_R), drift times (t_D), and flight times (t_F) in values of $t_R[t_D(t_F)]$ and units of min[ms(μs)]. In some cases, it is useful to describe individual $t_D(t_F)$ frames; in this case, the frame number multiplied by the acquisition time for each frame can be used to obtain the value of t_R. In the present system, we have used an acquisition delay of 10.0 min. This is effectively the time required for the first peptides to begin eluting off the column. Finally, it is also useful to convert flight times into m/z values. This is done with a standard

(19) Licklider, L. J.; Thoreen, C. C.; Peng, J.; Gygi, S. P. *Anal. Chem.* **2002**, *74*, 3076.

(20) Riddiford, L. M.; Cherbas, P.; Truman, J. W. *Vitamins Hormones* **2001**, *60*, 1.

(21) (a) Ji, J.; Chakraborty, A.; Geng, M.; Zhang, X.; Amini, A.; Bina, M.; Regnier, F. E. *J. Chromatogr., B* **2000**, *745*, 197. (b) Geng, M.; Ji, J.; Regnier, F. E. *J. Chromatogr., A* **2000**, *870*, 295.

(22) Recipe for Bloomington *Drosophila* food can be found in: http://flystocks.bio.indiana.edu/bloom-food.htm.

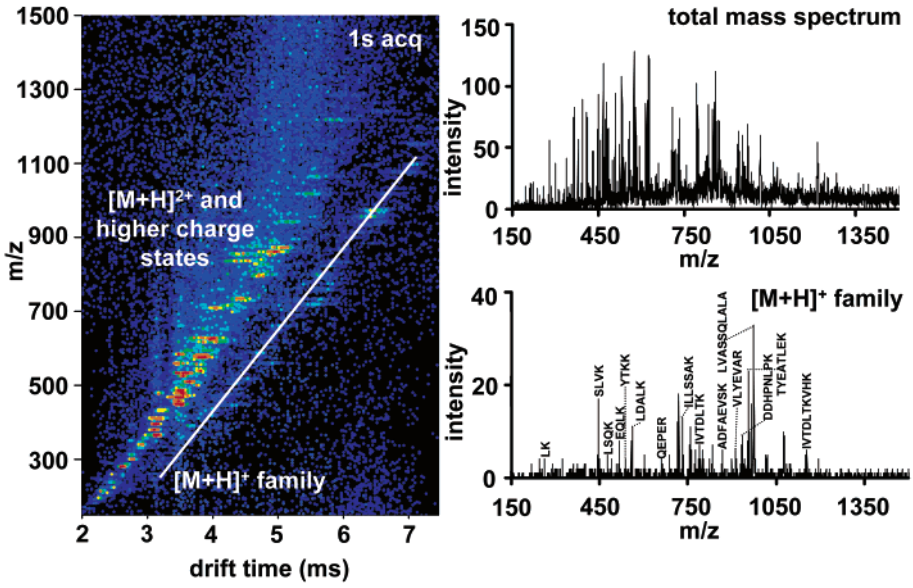

Figure 2. Two-dimensional plot (left) of drift times and *m*/*z* ratios for a digest of horse albumin. The intensity of different features is shown using a false color scheme in which the least intense features are represented in blue and the most intense features are represented in red. This data set was acquired upon electrospraying a 1.0 mg·mL^{-1} solution of the digest and acquiring data for 100 experimental cycles. The total acquisition time was 1.0 s. As described previously, peaks fall into families of $[M + H]^+$ (the series of relatively faint peaks, delineated by the solid white line) and $[M + 2H]^{2+}$ and higher charge state ions (the more intense features). The spectrum at the top right portion of the plot shows the total mass spectrum obtained by integrating each TOF window over the complete range of drift time bins. The bottom right spectrum corresponds to integration of the narrow range of $[M + H]^+$ ions along the solid white line. We note that even relatively small features are readily observed after only a short acquisition time. In all, ~100 peaks can be observed across the total mass spectrum. The inset shows only a few assignments for the $[M + H]^+$ family of ions. Many other peaks can be assigned to expected $[M + 2H]^{2+}$ and $[M + 3H]^{3+}$ tryptic peptides as well as some missed cleavages. A detailed analysis and assignment has been given previously (see ref 6).

multipoint calibration of a known sample. This calibration is usually taken before and after each LC-IMS-MS data set is acquired.

RESULTS AND DISCUSSION

Fast Acquisition of a Nested $t_D[t_F]$ Data Set for a Tryptic Digest of Albumin. It is worthwhile to start by showing an example data set for several relatively simple systems. Figure 2 shows a nested $t_D[t_F]$ data set obtained for a mixture of tryptic peptides from horse albumin. These data are obtained by electrospraying a 1.0 mg·mL^{-1} solution and acquiring data for 100 experimental cycles (a total acquisition time of 1.0 s). As described previously, ions fall into families according to their charge states. In total, we observe evidence for ~100 peaks (of which 15 can be assigned to peptides of albumin from the +1 charge-state family). Figure 2 also shows an integrated mass spectrum for the complete data set as well as a plot obtained by integrating along the family of $[M + H]^+$ peptides. A clear advantage of this approach is that many small $[M + H]^+$ peptides that are effectively buried under chemical noise in the complete mass spectrum can be clearly observed in the selected slice across the data set. We count ~25 peaks associated with $[M + H]^+$ ions. The ability to acquire data such as these in a 1.0-s acquisition time provides a direct assessment of the improvement associated with the incorporation of the octopole. We estimate that the signals have been increased by a factor of ~50−200 relative to that acquired with the analogous approach using a Paul geometry trap.[14]

Signal-to-Noise (S/N) Ratio of Measurements Associated with Electrospraying a Four-Component Peptide Mixture. An additional system (a simple peptide mixture that includes methionine enkephalin, angiotensin I, angiotensin II, and substance P) provides another important assessment of octopole. Hoaglund-Hyzer et al.[10] have previously reported detection limits (using the analogous Paul geometry instrument) of 17, 5, 3, and 4 fmol, for methionine enkephalin, angiotensin I, angiotensin II, and substance P, respectively, using nanospray tips. We have tested the new detection limits of this instrument upon inclusion of the octopole by direct infusion ESI of several solution concentrations. Figure 3 shows one nested $t_D[t_F]$ data set that was obtained consuming a total of 2.1 pg for each peptide (corresponding to consumption of 3.6, 1.6, 2.0, and 1.6 fmol of methionine enkephalin, angiotensin I, angiotensin II, and substance P, respectively). From these data we clearly observe peaks that can be assigned to the following ions: the $[M + H]^+$ ion of methionine enckphalin, at t_D $(m/z) = 5.6$ (573.7); the $[M + H]^{2+}$ ions of angiotensin II and substance P, at t_D $(m/z) = 4.4$ (1046.2), and 5.2 (1347.6), respectively; and, the $[M + H]^{3+}$ ions of angiotensin I, angiotensin II, and substance P at t_D $(m/z) = 4.0$ (1296.5), 3.4 (1046.2), and 3.6 (1347.6), respectively.

Although the S/N = 3 definition of a detection limit is unambiguous, one must use caution in how this is defined in multidimensional data such as those obtained here—primarily because the level of noise observed in these measurements depends heavily upon where it is measured. That is, if one were to integrate the signal across a narrow t_D (m/z) region of a peak to obtain S and integrate similar regions chosen randomly over regions where no peaks were present to obtain N, then different values for the detection limits would be obtained. This can lead to arbitrarily low detection limits. For example, there is essentially

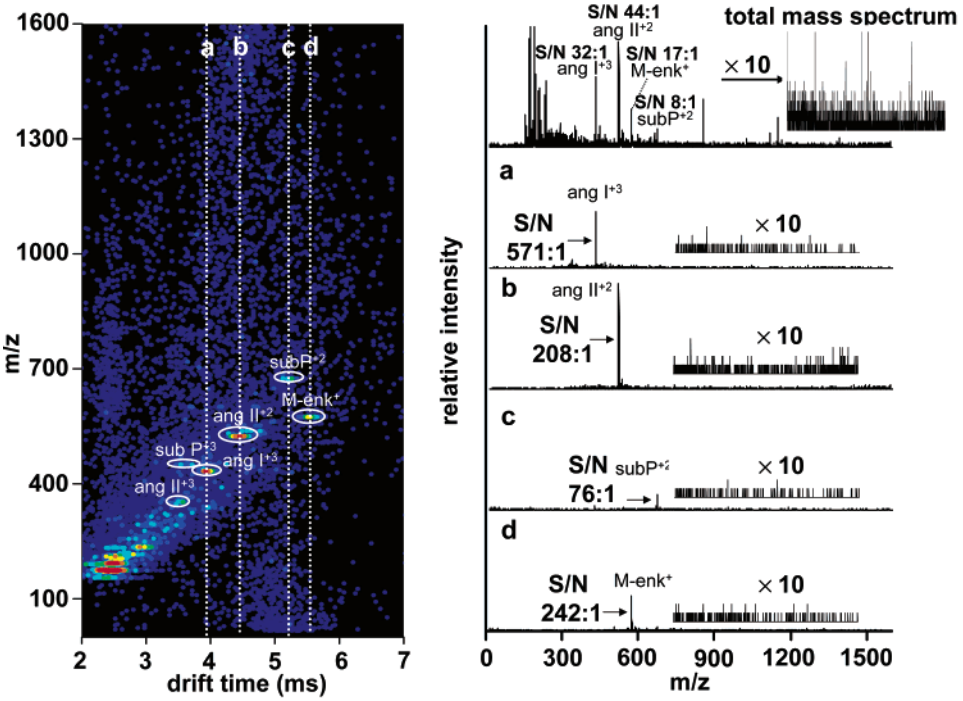

Figure 3. Two-dimensional plot (left) of drift time and *m*/*z* ratios for a well-defined four-component peptide mixture (angiotensins I and II, substance P, and methonine enkaplin). These data were acquired upon electrospraying 2.1 pg of each peptide. The total acquisition time was 10 s. The mass spectral plots shown to the right corresponds to integration of specific regions of the two-dimensional data set. The top right spectrum shows integration across all drift bins and corresponds to the complete mass spectrum. Note a significant level of noise is formed at short drift times. The baseline noise level for this spectrum between 700 and 1580 *m*/*z* is 1 count·bin^{-1}. Using this value, and the areas under each peak, we determine S/N = 32, 44, 17, and 8 for peaks corresponding to the $[\text{ang I} + 3\text{H}]^{3+}$, $[\text{ang II} + 2\text{H}]^{2+}$, $[\text{M-enk} + \text{H}]^{+}$, and $[\text{sub P} + 2\text{H}]^{2+}$ ions. Slices across peaks for individual ions taken at drift times 3.8, 4.4, 5.3, and 5.55 ms are also shown as mass spectral plots. These plots show a much lower noise level and S/N = 571, 208, 242, and 76 can be determined for the same respective ions. See text for details.

no noise over the region from $t_D = 6$ to 7 ms and $m/z = 100$ to 200, whereas the noise level associated with an analogous region size from $t_D = 2$ to 3 ms and $m/z = 700$ to 800 is much larger. This difference arises because of the nature of the drift tube separation; chemical noise appears to reside in specific locations of the spectrum. One expects this to be the case as most of the chemical noise in this system emerges from distributions of partially solvated clusters as well as other impurities in the sample. In the present dataset, the large unassigned features centered in the t_D (m/z) region of ~2.5 (300) appear to be related to the noise at higher m/z near this drift time.

Table 1 lists a representative estimate of the detection limits for this system. To estimate a representative value of N for this measurement, an area that was ~300 times greater than the area used to obtain S from specific peaks was sampled and subsequently normalized to the area of the signal. In each case, we take N at the same drift times as the parent peak that we are examining. For this study, a $t_D(t_F)$ distribution was acquired for 10 s for a mixture of four peptides at 1.0 ng·μL^{-1} at the nano flow rate of 50 nL·min^{-1}, using a homemade pulled capillary nanotip. As shown in Figure 3, the noise level associated with a specific drift time is a factor of ~10 times lower than the noise associated with the total mass spectrum. From the individual peaks in Figure 3, we determine S/N of 571, 208, 76, and 242 for the $[\text{M} + 3\text{H}]^{3+}$ ion of angiotensin I, the $[\text{M} + 2\text{H}]^{2+}$ ions angiotensin II and substance P, and the $[\text{M} + \text{H}]^{+}$ ion of methionine enkaphalin, respectively. This leads to an estimate of detection limits of 8, 29, 61, and 45 amol for these ions, respectively. These detection limits are a factor of 12 ± 5 lower than those obtained from the integrated mass spectrum for these data; additionally, these detection limits are lower by factors of 46−625 than those reported previously by Hoaglund-Hyzer using the Paul trap.[10]

Table 1. S/N of a 1.0 pg·μL^{-1} Four-Component Peptide Mixture

peptide ions	S/N[a]	DL (amol)[b]	S/N[c]	DL (amol)[d]
$[\text{Met-enkephalin} + \text{H}]^{+}$	242	45	17	646
$[\text{substance P} + 2\text{H}]^{2+}$	76	61	8	584
$[\text{angiotensin II} + 2\text{H}]^{2+}$	208	29	44	137
$[\text{substance P} + 3\text{H}]^{3+}$	101	46	12	390
$[\text{angiotensin I} + 3\text{H}]^{3+}$	571	8	32	152
$[\text{angiotensin II} + 3\text{H}]^{3+}$	93	65	6	1004

[a] S/N for parent ions were determined by series of studies carried out using the lowest concentration of 1.0 ng·μL^{-1} solution of a four-component peptide mixture (2.1 pg for each peptide). The noise was taken by integrating over the m/z range of 700−1580 for each narrow drift time range of the signal. The area of the signal was normalized to that of the signal area. See text for discussion. [b] Detection limits for the S/N on the left column. Values correspond to the amount of consumed sample that was required to produce S/N = 3. Detection limits were given in attomoles and estimated using DL = peak intensity (at S/N = 3) × total amount consumed (per peptide component)/peak intensity. [c] S/N for parent ion where noise was integrated over all drift time bins over the m/z range of 700−1580. [d] Detection limits for the S/N on the left column. Values correspond to the amount of consumed sample that was required to produce S/N = 3. Detection limit was calculated as mentioned above.

Example of a Nano-LC-IMS-TOF Separation of the GIST Labeled *Drosophila* Fly Proteome. The improvements that

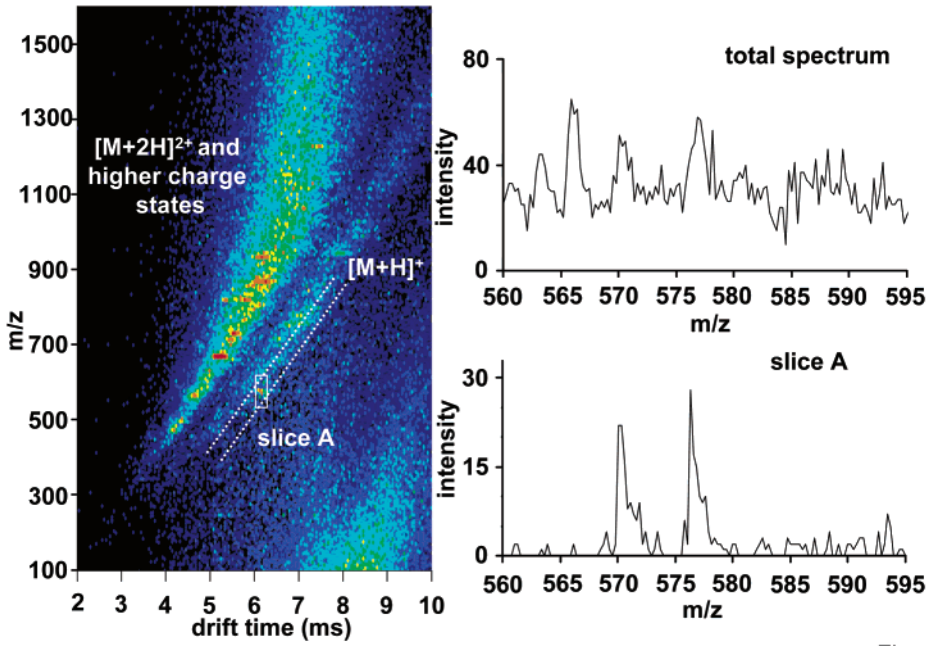

Figure 4. Individual two-dimensional IMS-TOF frame (left) acquired for 0.16 min during a nano-LC-IMS-TOF separation of GIST labeled tryptic peptides from nonstimulated cells; the total mass spectrum, obtained by integration across all drift time bins from *m*/*z* 560 to 595 s shown at the top right. The same range corresponding to only a few bins over the same range, which includes only $[M + H]^+$ ions, is also shown (bottom right). Note that the ratio of light and heavy isotopically labeled ions is readily determined from the latter spectrum. (Left) Nested $t_D(t_F)$ distribution at retention time of ~47 min from the nano-LC-IMS-TOF experiment of *Drosophila* proteome. (Right) Total mass spectrum and mass spectrum for the box A were shown. See text for details.

have been reported now make it possible to extend the nested $t_D[t_F]$ measurements for the analysis of complex proteome mixtures for the first time. Here, we provide examples of two types of studies that we have conducted. These systems are under detailed investigation in our laboratory, and a complete analysis of these data will be given elsewhere.

A preliminary study of the ecdysone induced and normal *Drosophila* proteins that have been digested with trypsin and labeled using the GIST method[21] has been carried out. In this experiment, ~1.0 μg of total protein was injected onto a nano-LC column that was coupled to the octopole trap-IMS-TOF instrument. Nested $t_D(t_F)$ distributions were recorded every 10 s for 90 min as peptides eluted from the column. A visual inspection of a small fraction of the total frames recorded for the normal *Drosophila* proteins, as shown in Figure 4, allows us to estimate that we have detected between 3×10^3 and 3×10^4 different peptide ions for the entire data set. Note that the lower value is a very conservative limit. A more detailed analysis will be presented elsewhere.

Figure 4 shows one $t_D(t_F)$ distribution within this data set; this distribution was obtained at retention time of ~47 min. As is typical of most $t_D(t_F)$ frames across the data set, we observe evidence for multiple charge-state families; here, the $[M + H]^+$ family of peptide ions is resolved from the $[M + 2H]^{2+}$ and higher charge-state ions. Integration across all drift times gives the total mass spectrum (also shown over the region from $m/z = 560$ to 595), and integration across the region associated with the $[M + H]^+$ family gives the mass spectrum associated with singly charged peptides (also shown). A comparison of these mass spectra allows us to illustrate the advantage associated with detecting the abundances of GIST labeled peptide pairs. Here, the light and heavy isotopes of the $[M + H]^+$ peptide are clearly apparent when the large chemical noise associated with the $[M + 2H]^{2+}$ and higher charge-state ions is removed. This result would not be possible to obtain (at our current TOF resolution) by MS alone.

Example of a Nano-LC-IMS-TOF Separation of Tryptic Peptides Obtained from Digesting Proteins from the Head of a Single *Drosophila* Fly. A second example is shown in order to illustrate the advantages associated with a combined LC−IMS separation. In this case, we have extracted proteins from a single fly head[23] and analyzed their tryptic digest. In this approach, we have injected ~0.5 μg of peptides onto a homemade nano-LC column and each $t_D(t_F)$ frame obtained within the complete $t_R[t_D(t_F)]$ data set (obtained over ~130 min) was recorded for 5 s. Figure 5 shows a plot of the two-dimensional $t_R[t_D]$ separation. This plot is obtained by integrating the ion intensity across all flight times (i.e., all values of t_F). The complexity of this sample is such that many peptides appear to elute across all retention times. Overall, most of the signal associated with this data set appears to fall along a broad partially resolved feature that extends from frames 200 to 1200 (low-intensity features are observed between frames 1200 and 1400); an additional feature that begins near frame 1500 is associated with a rapid solvent wash of the column that is done to remove any highly retained peptides. A blowup of a region of this plot that provides a better feeling about the shapes of specific features is also shown in Figure 5. This plot shows that many of the features that could not be resolved with the LC separation alone do appear to be at least partially resolvable with the combined LC−IMS separation.

It is interesting to examine the mass spectra for some of these peaks. We have arbitrarily chosen six points along the LC−IMS separation to examine in more detail, and the mass spectral dimension is shown for each of these regions. Overall, these plots

(23) Diederich, R. J.; Pattatucci, A. M.; Kaufman, T. C. *Development* **1991**, *113*, 273.

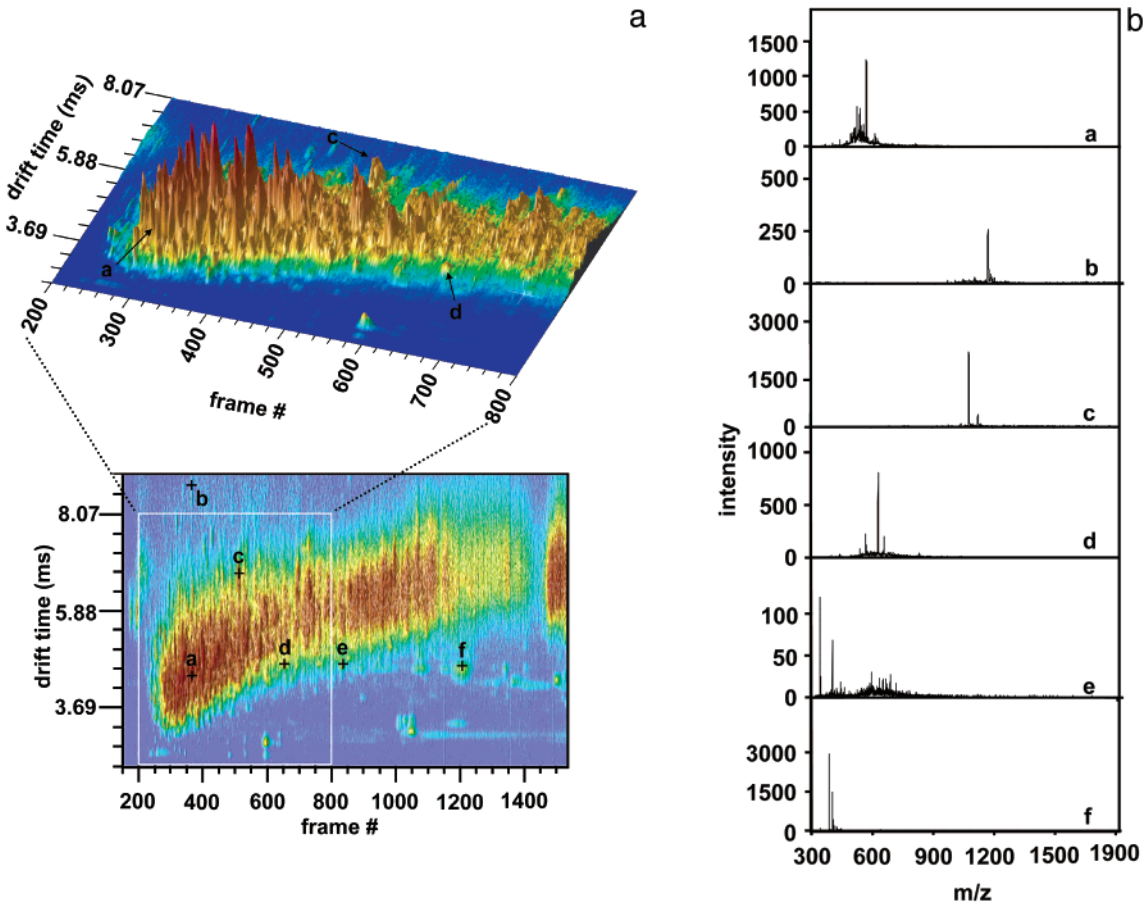

Figure 5. (a) Nano-LC−IMS-TOF distribution recorded for a mixture of tryptic peptides obtained from proteins extracted from a single *drosophila*'s head. These data comprise a complete nano-LC-IMS-TOF separation in which each two-dimensional IMS-TOF data set is referred to as a frame. The plot shows frames 175−1525. Each two-dimensional IMS-TOF frame was recorded for 5 s. The distribution of features that are observed at different drift times corresponds to species that were not separated using only the LC column. A zoomed area (frames 200−800) is shown on top of (a) as a mountain plot. The data set is positioned at a different angle to display the intensities that are acquired by integrating over the t_F dimension. (b) shows the mass spectra that are obtained for each of the regions labeled using a "+" in (a). The six mass spectra displayed reveal that in some cases only a few ions are present at each frame/drift time value; however, in other regions, many ions may still be present after both transitions of separations.

show that some features (e.g., b, c, and f) appear to correspond to only a few components; others features in the LC−IMS plot, such as a, d, and e may still contain many components. For example, a careful examination of the mass spectrum from region e shows more than 25 resolvable peaks.

One final point is associated with the dynamic range of this approach. Examination of a number of mass spectra shows that peak intensities of <10 ions can be resolved and reliably reported; the largest peaks appear to contain more than 10^5 ions (the integrated signal across a peak); thus, from our preliminary study, it appears that, even in this very complicated sample, this system will offer a dynamic range of $\sim 10^3-10^4$. We are currently investigating the dynamic range in more detail.

Current Limitations. While the current advances offer significant improvements in detection limits and the ability to address real proteome systems for the first time in a rapid fashion, a number of factors are still limiting our instrumentation. Some of these factors (such as limitations in source efficiency and relatively low (compared with commercial instruments) time-of-flight duty cycle and resolving power) arise from the fact that this is a home-built instrument and these parameters have not been optimized. Another issue involving how to analyze such large data sets is clearly apparent, and the limited analysis that is given for the LC-IMS-TOF data that are shown clearly reflects this limitation. We are currently in the process of writing code to automate data analysis; however, a fully automated approach will require significant work and is still some time away.

Another interesting problem that we did not anticipate is associated with detector saturation. Current ion signals at our detectors are much higher than in our previous reports, and ions reach the detector in relatively sharp packets (associated with their separation through the drift tube) rather than continuously (as is typically the case in ESI-TOF instruments). Consider, for example, a single ion that is dispersed into the TOF instrument from an on-axis beam of $\sim 10^7$ ions·s^{-1} at 1% efficiency. A conventional TOF instrument that acquires data at 10^4 Hz would need to record 10 ions per experiment—a challenging but manageable problem. The same measurement of a single m/z ion in our system having the same on-axis signal and the same TOF duty cycle becomes significantly more challenging because the continuous signal now arrives in a short packet (substantially less than 1 ms at fwhm). In this case, our time-to-digital detector saturates and we do not accurately record the shape of the peak. This is now the case that we observe upon electrospraying typical solutions in our

laboratory; one way to approach this problem is to decrease solution concentrations that are used for ESI. We currently have done this; we are also working on a new more efficient detector for this instrument.

SUMMARY AND CONCLUSIONS

We have shown that the implementation of a linear octopole ion trap can have a significant impact on our IMS-TOF instrumentation. It appears that signals are improved by factors of ∼50−200 compared with our analogous Paul trap configuration.[14] With these improvements it is possible to record nested $t_D(t_F)$ data sets on short time scales (routinely <1.0 s); additionally, detection limits in the 10−100-amol range are accessible. An important application that is associated with this advance has been demonstrated. For the first time, we report three-dimensional LC-IMS-MS separations of a whole proteome. This system that we have chosen to demonstrate this approach is the *Drosophila*; we illustrate an advantage in defining groups of GIST labeled peptides and also have shown results from the analysis of a single fly head. The increased signals bring about new challenges associated with detector saturation and the issue of how to manage such a large data set; we are working on a new detection system to overcome the former problem and are beginning to develop software for the analysis of 3D data sets.

ACKNOWLEDGMENT

This work is supported by grants from the National Science Foundation (CHE0078737) and National Institute of Health (1R01GM-59145-03). We are also grateful for support from the Indiana Genomics Initiative (INGEN), which has funded some other instrument development in our group that is related to this work and has helped us to develop the collaborations associated with this work. Y.J.L. and M.H.M. were supported under the INGEN funds. Finally, we are grateful to Dr. Xinfeng Gao and C. Ray Sporleder for their help in graphic visualization of these data.

Received for review March 17, 2003. Accepted July 17, 2003.

AC030107F